

Two Fermion Production at LEP II

P. J. Holt

*Department of Physics, NAPL, Keble Road,
Oxford OX1 3RH, England*



The measurements of the LEP collaborations on the process $e^+e^- \rightarrow f\bar{f}$ at centre-of-mass energies above the Z resonance from 130 - 189 GeV are summarised. Examples of the interpretation of the results within the Standard Model and in models which introduce physics beyond the Standard Model are given.

1 Introduction

The LEP Collaborations, ALEPH, DELPHI, L3 and OPAL, have made studies of two fermion production at LEP II, including preliminary studies of data collected in 1998 at a centre-of-mass energy (\sqrt{s}) of approximately 189 GeV, with an average integrated luminosity of about 170 pb^{-1} per experiment.

In the Standard Model (\mathcal{SM}) at Born level observables for the process $e^+e^- \rightarrow f\bar{f}$ are simple to predict, depending on the exchange of Zs and photons. The cross-sections for $e^+e^- \rightarrow f\bar{f}$ is some 2-3 orders of magnitude smaller than that at LEP I energies, $\sqrt{s} \sim M_Z$, while the forward-backward asymmetry^a is larger than at the Z resonance. Large radiative corrections come from the process of radiative return in which initial state photons are emitted reducing the invariant mass of the $f\bar{f}$ system ($\sqrt{s'}$) to approximately M_Z . These corrections approximately double the total cross-section, while diluting the forward-backward asymmetry.

In addition to the \mathcal{SM} exchanges, physics beyond the Standard Model could contribute to the matrix elements. The data can be used to search for, or put limits on, such effects.

In what follows the measurements by the four LEP collaborations are summarised, followed by examples of the results obtained for different interpretations of the data. For a more exhaustive summary of the interpretations of the data readers should refer to the publications of the LEP collaborations^{1,2,3,4} and submissions to conferences⁵

2 Measurements of $e^+e^- \rightarrow f\bar{f}$

The LEP experiments have published measurements of the process $e^+e^- \rightarrow f\bar{f}$ ^{1,2,3,4} and have given preliminary results based on data taken at $\sqrt{s} \sim 189 \text{ GeV}$ with an average luminosity of approximately 170 pb^{-1} per experiment.⁵

The event selections are rather similar to those used by the LEP experiments at Z energies⁶ They must be slightly modified to take into account falling signal cross-section and increasing backgrounds such as two-photon collisions and four fermion processes, in particular $e^+e^- \rightarrow W^+W^-$ and $e^+e^- \rightarrow ZZ$. It is also necessary to be efficient for radiative return topologies, in which there tends to be missing energy carried away down the beam pipe by an initial state photon, leaving the fermions highly acollinear.

The collaborations also have to estimate the invariant mass of the final state fermions, this can be determined solely from the angles of the fermions assuming a single photon is emitted along the beam pipe:

$$\frac{\sqrt{s'}}{\sqrt{s}} = \frac{\sin \theta_f + \sin \theta_{\bar{f}} - |\sin(\theta_f + \theta_{\bar{f}})|}{\sin \theta_f + \sin \theta_{\bar{f}} + |\sin(\theta_f + \theta_{\bar{f}})|}$$

In practice the collaborations use more complex algorithms, the details of these are different for different final states and different collaborations, but typical inputs include the measured energy in the fermion system and the angles between the fermions, and also the four vectors of any photons identified within the detectors.

The collaborations report cross-sections for e^+e^- , $\mu^+\mu^-$, $\tau^+\tau^-$ and hadronic states and forward-backward asymmetries for the leptonic final states. These results are each given for two ranges of invariant mass: Non radiative events, $\sqrt{s'} > (0.85 - 0.90)\sqrt{s}$, where the invariant mass is close to the centre of mass energy of the collisions; and a more inclusive sample which also includes radiative return events, $\sqrt{s'} > 0.10\sqrt{s}$ or $\sqrt{s'} > 75 \text{ GeV}$. The approximate statistical precision on cross-sections obtained in the various channels is summarised in table 1. At this level of precision, systematic errors start to become similar to the statistical errors. The experimental errors should be compared

^a The forward-backward asymmetry, A_{FB} , is defined as: $(N_f - N_b)/(N_f + N_b)$, where N_f and N_b are the number of events where the outgoing fermion travels into the same hemisphere as the direction of the incoming electron and positron respectively.

^b $\sqrt{s'}$ is sometimes related to the effective centre of mass energy of the hard collision, this involves distinguishing between initial and final state radiation which is not well defined because of interference at the amplitude-squared level between the two types of radiation.

Sample	Hadrons	$\mu^+\mu^-$	$\tau^+\tau^-$
Non Radiative	0.7%	3%	4%
Inclusive	2%	5%	6%

Table 1: The approximate statistical precision on the cross-section measurements obtained in the hadronic, $\mu^+\mu^-$ and $\tau^+\tau^-$ channels with data collected at $\sqrt{s} \sim 189$ GeV in 1998

to the theoretical uncertainty which comes mainly from radiative corrections and is estimated to be $\mathcal{O}(1\%)$. Care is needed when comparing cross-sections and forward-backward asymmetries between experiments - DELPHI scale hadronic, $\mu^+\mu^-$ and $\tau^+\tau^-$ results to 4π acceptance, whereas OPAL have in the past quoted numbers, applying a correction for interference between initial and final state interference.

The preliminary measured cross-sections and asymmetries at $\sqrt{s} \sim 189$ GeV agree well with the predictions of the Standard Model.

3 Interpretations of the data

3.1 S-Matrix

In the S-Matrix formalism the cross-sections and forward-backward asymmetries are parameterised in terms of the exchange of a massless and a massive neutral boson (the photon and the Z) as follows:

$$\begin{aligned}\sigma_{tot}^0(s) &= \frac{4}{3}\pi\alpha^2 + \left[\frac{g_f^{tot}}{s} + \frac{j_f^{tot}(s - \bar{m}_Z^2) + r_f^{tot}s}{(s - \bar{m}_Z^2)^2 + \bar{m}_Z^2\bar{\Gamma}_Z^2} \right] \\ \sigma_{fb}^0(s) &= \frac{4}{3}\pi\alpha^2 + \left[\frac{g_f^{fb}}{s} + \frac{j_f^{fb}(s - \bar{m}_Z^2) + r_f^{fb}s}{(s - \bar{m}_Z^2)^2 + \bar{m}_Z^2\bar{\Gamma}_Z^2} \right] \\ A_{fb}^0(s) &= \frac{3}{4} \frac{\sigma_{fb}^0(s)}{\sigma_{tot}^0(s)}\end{aligned}$$

The parameters g , j and r are independent. In the Standard Model these parameters are related to each other via the couplings of the Z and the photon to the final state f and can be predicted. In particular the parameter j_{had}^{tot} represents the contribution of the interference of the Z and the photon to the total hadronic cross-section, a term which is constrained in the Standard Model. Using the quasi-model independent S-Matrix formalism it is possible to check that this term has the expected magnitude. Using LEP I and LEP II data L3 obtain a preliminary value of:

$$j_{had}^{tot} = 0.29 \pm 0.13.$$

This should be compared with the result of the analysis of VENUS and LEP I data:⁷

$$j_{had}^{tot} = 0.20 \pm 0.08.$$

The Standard Model expectation is

$$j_{had}^{tot} = 0.22 \pm 0.01.$$

3.2 Contact Interactions

Four fermion contact interactions parameterise physics beyond the Standard Model with an effective Lagrangian :

$$\mathcal{L}_{eff} = \frac{g^2}{(1 + \delta_{ef})\Lambda^2} \sum_{i,j=L,R} \eta_{ij} \bar{e}_i \gamma_\mu e_i \bar{f}_j \gamma^\mu f_j,$$

⁷The definition of \bar{m}_Z is slightly different to the standard definition of M_Z in the usual Standard Model fits which take into account the energy dependence of the width term in the Z propagator.

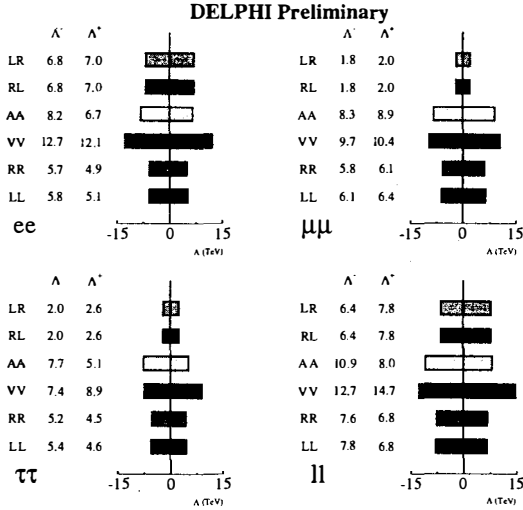


Figure 1: Limits from DELPHI on the energy scale, Λ of contact interactions for different final states, e^+e^- , $\mu^+\mu^-$, $\tau^+\tau^-$ and l^+l^- , the average of the three separate final states, for different helicity structures (LL, RR, etc) with constructive (+) and destructive (-) interference with the Standard Model.

$$\delta_{ef} = \begin{cases} 1 & f = e \\ 0 & f \neq e \end{cases}$$

which introduces a characteristic high energy scale Λ .⁸ Different models assume different values for each of the 4 helicity couplings η_{ij} with either constructive (+) or destructive (-) interference with the Standard Model. Fits to data on $e^+e^- \rightarrow f\bar{f}$ are performed assuming $g^2/4\pi = 1$, with the free parameter $\epsilon = 1/\Lambda^2$, where $\epsilon = 0$ in the limit of no contact interactions. No evidence is found for contact interactions and 95% confidence limits on the energy scale have been produced. The results from DELPHI for leptonic final states are summarised in figure 1. The data at $\sqrt{s} \sim 189$ GeV leads to an increase in the limits for the average of $e^+e^- \rightarrow l^+l^-$ by 1.6 - 6.2 TeV depending on the helicity structure assumed.

3.3 R-Parity Violating Supersymmetry

In \mathcal{R} supersymmetry two terms in the superpotential are relevant to $e^+e^- \rightarrow f\bar{f}$ at LEP II,⁹ purely leptonic terms:

$$\lambda_{ijk} L_L^i L_L^j \bar{E}_R^k$$

and lepton-quark terms:

$$\lambda'_{ijk} L_L^i Q_L^j \bar{D}_R^k$$

where ijk are generation indices, L_L and Q_L represent left-handed superfield doublets of leptons and quarks while \bar{E}_R and \bar{D}_R correspond to the right-handed singlet superfields of charged leptons and down like quarks. The couplings λ_{ijk} and λ'_{ijk} are only non-zero for combinations involving at least two generations and for $i < j$. Depending on which of the couplings λ_{ijk} and λ'_{ijk} take non-zero values it is possible to have s and/or t channel exchange of $\bar{\nu}$ or \bar{q} .

From s -channel exchange it is possible to put limits on $\lambda_{ijk}^{(l)}$ as a function of the exchanged sfermion mass. Exclusion limits from L3 for the $e^+e^- \rightarrow e^+e^-$ and $e^+e^- \rightarrow \mu^+\mu^-$ channels are shown in figure 2,

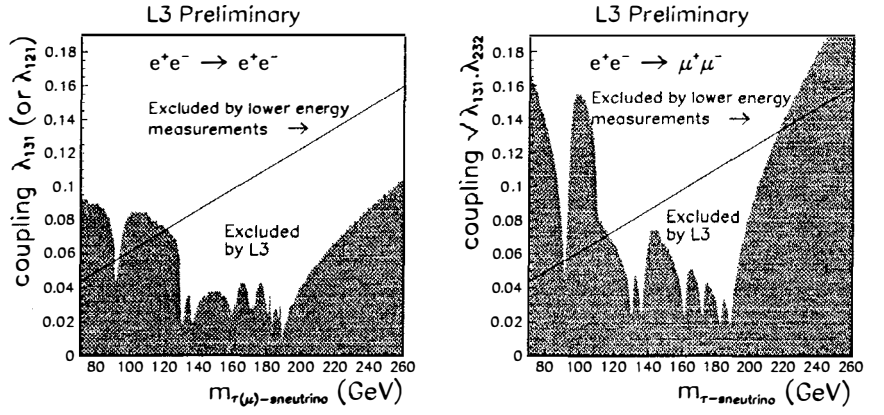


Figure 2: 95% exclusion limits from L3 on couplings λ'_{jk} in \tilde{R} supersymmetry for the $e^+e^- \rightarrow e^+e^-$ and $e^+e^- \rightarrow \mu^+\mu^-$ channels as a function of sneutrino mass.

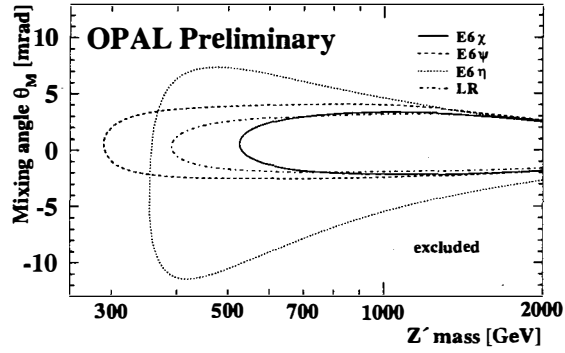


Figure 3: 95% exclusion limits on $M_{Z'}$ and $\theta_{ZZ'}$ for four Z' models from OPAL.

assuming non-zero couplings are equal, the following limits are obtained at 95% confidence:

$$\lambda_{ijk} \lesssim 0.03 \text{ for } 120 < m_{\tilde{\nu}} < 190 \text{ GeV.}$$

3.4 Leptoquarks

Leptoquarks are fractionally charged particles which are classified by their spin, weak isospin, hypercharge and the chirality of their couplings. The exchange of certain leptoquarks would be identical to the exchange of particular squarks in \tilde{R} supersymmetry,⁹ for example: $\tilde{d}_R \leftrightarrow S_{0(L)}$ and $\tilde{u}_L \leftrightarrow \tilde{S}_{1/2}$.

Assuming a coupling of $\sqrt{4\pi\alpha}$ ALEPH obtain an indirect limit on the mass of a $S_{0(L)}$ of $M > 310$ GeV.

3.5 Z' Bosons

Many extensions to the Standard Model predict new neutral, massive bosons collectively known as Z' 's, having a mass $M_{Z'}$. These bosonic fields can mix with the standard Z with a mixing angle $\theta_{ZZ'}$. Exchange of a Z' would affect the cross-sections and forward-backward asymmetries. Within particular models the couplings of the Z' to fermions are determined, and limits can be put on the mass and the

	M_s (TeV)		
	$\mu^+\mu^-$	$\tau^+\tau^-$	l^+l^-
+	0.58	0.63	0.65
-	0.65	0.50	0.64

Table 2: 95% limits from OPAL on the scale M_s in quantum gravity for $e^+e^- \rightarrow \mu^+\mu^-$, $e^+e^- \rightarrow \tau^+\tau^-$ channels and $e^+e^- \rightarrow l^+l^-$, the average of the two individual channels for constructive (+) and destructive (-) interference with the Standard Model.

mixing angle of the Z' . Two dimensional 95% confidence level exclusion limits from OPAL are shown in figure 3. At 95% confidence level the one dimensional limits on the Z' mass are:

Model	χ	ψ	η	LR
$M_{Z'} > (\text{GeV})$	589	307	392	419

Limits typically improve by ~ 70 with the inclusion of data at $\sqrt{s} \sim 189$ GeV.

In the sequential Standard Model the Z' has exactly the same couplings as the standard Z . In this model ALEPH obtains a limit of $M_{Z'} > 1050$ GeV, which can be compared with the direct limit of CDF;¹⁰ $M_{Z'} > 690$ GeV.

3.6 Graviton exchange

It has recently been pointed out that the quantum gravity scale, M_D , could be of the order of the electroweak scale, M_{EW} , i.e. $\ll M_{Planck}$,¹¹ provided there are a total of $D = n + 4$ dimensions, n of which are compactified with a radius, R , given by:

$$R^n M_D^{n+2} = M_{Planck}^2$$

It cannot be excluded that this radius is as large as 1 mm, which would give $M_D \sim M_{EW}$ for $n = 2$.

In the process $e^+e^- \rightarrow f\bar{f}$ a large number of graviton modes would be radiated in these compactified dimensions, giving sizeable changes to observables in $e^+e^- \rightarrow f\bar{f}$. In high energy collisions, the gravitational interaction should be flavour independent, as gravity couples to the energy and momentum tensor. The expected change to the differential cross-section has the form:

$$\frac{d\sigma}{d\cos\theta} = A(\cos\theta) + B(\cos\theta) \left[\frac{\lambda}{M_s^4} \right] + C(\cos\theta) \left[\frac{\lambda}{M_s^4} \right]^2.$$

Where A is the Standard Model angular distribution and B, C are quartic power series in $\cos\theta$, representing the additional contributions from graviton modes. M_s is a scale of order M_D .

OPAL have studied the $e^+e^- \rightarrow \mu^+\mu^-$ and $e^+e^- \rightarrow \tau^+\tau^-$ channels taking $\lambda = \pm 1$ and fitting $\epsilon = 1/M_s^4$, obtaining the limits on M_s shown in table 2.

Acknowledgements

The author would like to thank members of the ALEPH, L3 and OPAL collaborations for their help in providing material for presentation at the XXXIV Rencontre de Moriond.

References

1. ALEPH Collaboration, D. Buskulic *et al*, Phys. Lett. **B378** (1996) 373.
ALEPH Collaboration, R. Barate *et al*, Phys. Lett. **B399** (1997) 329.
ALEPH Collaboration, R. Barate *et al*, CERN-EP/99-042.
2. The DELPHI Collaboration, P. Abreu *et al*, CERN-EP/99-05.
3. L3 Collaboration, M. Acciarri *et al*, Phys. Lett. **B370** (1996) 195.
L3 Collaboration, M. Acciarri *et al*, Phys. Lett. **B407** (1997) 361.

4. OPAL Collaboration; G. Abbiendi *et al* , Euro. Phys. J. **C6** (1999) 1.
OPAL Collaboration; K. Ackerstaff *et al* , Euro. Phys. J. **C2** (1998) 441.
5. Contributions to winter conferences in 1999 and other conferences can be found from links on the web pages of the LEP Collaborations.
6. The ALEPH Collaboration, D. Buskulic *et al* , Z. Phys. **C62** (1994) 539.
The DELPHI Collaboration, P. Abreu *et al* , Nucl. Phys. **B418** (1994) 403.
The L3 Collaboration, M. Acciarri *et al* , Z. Phys. **C62** (1994) 551.
The OPAL Collaboration, R. Akers *et al* , Z. Phys. **C61** (1994) 19.
7. The VENUS Collaboration, K. Yusa *et al* , Phys. Lett. **B447** (1999) 167.
8. E. Eichten *et al* , Phys. Rev. Lett. **50** (1983) 811.
9. J. Kalinowski *et al* , Z. Phys. **C74** (1997) 595.
10. The CDF Collaboration, F Abe *et al* , Phys. Rev. Lett. **79** (1997) 2192.
11. G. F. Giudice *et al* , CERN-TH/98-354.